Performance Analysis of a 2-Link Haptic Device with Electric Brakes

Changhyun Cho
Advanced Robotics Research Center, KIST / Dept. of Mechanical Eng., Korea University, Seoul, Korea
chcho@kist.re.kr

Munsang Kim
Advanced Robotics Research Center Korea Institute of Science and Technology (KIST), Seoul, Korea
munsang@kist.re.kr

Jae-Bok Song
Dept. of Mechanical Eng., Korea University, Seoul, Korea
jbsong@korea.ac.kr

Abstract

Passive haptic devices have better stability than active ones, but usually have limited capability of haptic display. In this paper a 2-link passive haptic device equipped with electric brakes is discussed. Since passive devices cannot generate forces in all directions, determination of the region available for force reflection is important to their design and operation. This analysis can be done by a so-called force manipulability ellipsoid (FME). In some haptic applications, the endpoint of a device is required to move along a certain trajectory (e.g., the surface of a virtual wall) and haptic display plays a role of path guide. Performance of path guidance is also investigated in this research. Finally, guideline for the design of more efficient passive haptic devices is briefly discussed.

1. Introduction

An active actuator such as an electric motor is widely used in a device for haptic display as a force or torque generating actuator. Its weakest point is that it can generate supplementary energy to both a human operator and its feedback environment. Passivity control schemes for reducing internal energy in a haptic device are used for motor-driven haptic display devices in [1]. Even though stability problems of haptic devices with active elements can be solved using various control schemes, there remain mechanical problems due to size and weight of active actuators.

Compared with active haptic devices, research on passive haptic devices is rare [2, 3, 4, 8]. It was claimed in [2] that a brake can provide very hard constraints but it poses difficulty in control due to its passive characteristics. A nonholonomic haptic display adopting the constraint of a wheel (i.e., a wheel cannot rotate in the axial direction) is presented on [2]. [3] presented the single degree of freedom controller (SDOF Controller), which uses SDOF line achieved by locking one clutch to reduce a system DOF. The force manipulability ellipsoid (FME) for a haptic device equipped with passive actuators such as a brake and a damper was used in design procedure in [4].

Though passive haptic devices usually show relatively poor performance in comparison with the active ones on force display, it has significant benefits. The most papers say that safety can be greatly improved in passive devices, because motions are only initiated by user's inputs (i.e., force or velocity). Thus they cannot exert any harmful forces to a user.

The most important drawback of passive haptic display is that it cannot cover all force directions. This limitation can be investigated on force domain from the viewpoint of force manipulability, which is force-generating capability of a manipulator in task (or operational) space [5]. To systematically represent this capability, a so-called force manipulability ellipsoid (FME) is usually employed. An FME is a graphical representation of producible forces of a given mechanism in task space for a given kinematic configuration and can tell the capability of passive haptic devices.

In this paper, force manipulability analyses of typical 2-link manipulators are performed to find characteristics of a passive haptic display. The rest of this paper is organized as follows. A passive haptic display of a single DOF bar mechanism is investigated in Section 2. A brief introduction of FME is presented in Section 3. An FME of a typical 2-link manipulator is evaluated in Section 4 and its delimiting forces are investigated in Section 5. Design issues are discussed in Section 6. Conclusions are drawn in Section 7.

2. Haptic display by passive 1 DOF link

Figure 1 shows a single DOF link in contact with a virtual wall. A human operator applies a torque τ_H on the link through the handle and a passive actuator (e.g., electric brake) placed at the pivot point O exerts a control torque τ_C on the link. Since the passive actuator can only dissipate energy, τ_C is generated only against link rotation.

Proceedings of the11th Symposium on Haptic Interfaces for Virtual Environment and Teleoperator Systems (HAPTICS'03)
0-7695-1890-7/03 $17.00 © 2003 IEEE

When the endpoint comes in contact with the wall, it is deflected Δx by τ_H. During this wall deformation, the control torque τ_C is generated by a brake to provide the reaction force effect of a virtual wall. The magnitude of τ_C is commanded by a desired torque τ_{Cd} which is computed by a simple spring model.

$$\tau_{Cd} = -(k\Delta x)\cdot(l\cos\theta) \tag{1}$$

The equation of motion for this device is given by

$$I\ddot{\theta} = \tau_H + \tau_C \tag{2}$$

where I is the moment of inertia of the link about O.

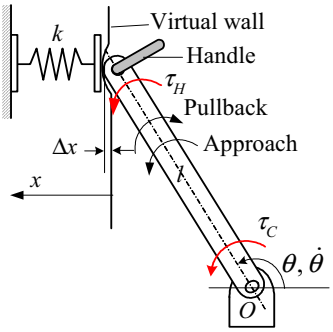

Figure 1. Virtual wall display with passive 1 DOF link

Control torque τ_C during contact with the wall can be described by the following passive constraint based on the stick-slip model [6]:

i) Slip mode (i.e, $|\dot{\theta}| \geq \delta\dot{\theta}$)

$$\tau_C = \begin{cases} -\mathrm{sgn}(\dot{\theta})|\tau_{Cd}| & \text{if } \mathrm{sgn}(\dot{\theta}) \neq \mathrm{sgn}(\tau_{Cd}) \\ 0 & \text{else} \end{cases} \tag{3}$$

ii) Stick mode (i.e., $|\dot{\theta}| < \delta\dot{\theta}$)

$$\tau_C = \begin{cases} -\tau_H & \text{if } \mathrm{sgn}(\tau_H) \neq \mathrm{sgn}(\tau_{Cd}) \\ 0 & \text{else} \end{cases} \tag{4}$$

where $\delta\dot{\theta}$ is a very small velocity value within which the stick mode is assumed. Equation (3) (or (4)) indicates that τ_C always acts in the direction opposite to rotation (or input torque).

Motion of 1 DOF link can be divided into three cases: free motion, approach, and pullback. In free motion, haptic display is not necessary and thus $\tau_C = 0$. During the approach and pullback motion where wall deformation occurs, the sign of τ_{Cd} determined by Eq. (1) is negative for both motions (i.e., $\tau_{Cd} < 0$) since the spring remains compressed. During approach, the brake is activated so that $\tau_C = -|\tau_{Cd}|$ to provide haptic effect. If the brake is still in action during pullback, however, it will prevent the user's pullback motion, so τ_C should be set to zero. This is ensured by the 2nd condition of Eq. (3) because $\dot{\theta} < 0$ and $\tau_{Cd} < 0$.

Now consider the stick mode. During approach, as the deformation continues, τ_C also increases and eventually becomes $-\tau_H$ and then the endpoint comes to a stop (i.e., stick mode). If this happens, the user cannot move the link in either direction because the brake is in action. The user is not able to perform a pullback motion because of the locked joint, which is not desirable. Therefore, the control torque τ_C should be set to zero when pullback motion is detected (by the 2nd condition of Eq. (4)). Since τ_H becomes negative for pullback motion, its detection is performed by sensing the joint torques.

From Eq. (3) and (4), one can easily imagine that the passive device cannot display a stored energy in the virtual spring. A brake can only stop the motion and cannot rotate a link in the opposite direction of motion. In the light of stability, this feature is beneficial because of no bouncing or overshoot behavior. Of course, insufficient capability of haptic display is a weak point of the passive haptic device. In this research, Eq. (3) and (4) is termed as the constraint equation of a passive actuator (in short, the passive constraint) for the case of haptic display.

3. Force manipulability ellipsoid

Consider a manipulator with n degrees of freedom (DOFs). The n-dimensional joint torque vector $\boldsymbol{\tau}$ is given by

$$\boldsymbol{\tau} = \mathbf{J}(\mathbf{q})^T \mathbf{F} \tag{5}$$

where $\mathbf{J}$ is the manipulator Jacobian matrix, $\mathbf{q}$ is the n-dimensional joint variable vector, and $\mathbf{F}$ is the m-dimensional endpoint force vector, respectively. For any arbitrary endpoint force $\mathbf{F}$, the joint torques $\boldsymbol{\tau}$ are always determined uniquely. Now consider a set of all endpoint forces $\mathbf{F}$ that are realizable by joint torques whose Euclidean norm satisfies the condition $\|\boldsymbol{\tau}\| = (\tau_1^2 + \cdots + \tau_n^2)^{1/2} \leq 1$. Applying this condition to Eq. (5) yields

$$\mathbf{F}^T\mathbf{J}\mathbf{J}^T\mathbf{F} \leq 1 \tag{6}$$

The set of endpoint forces given by Eq. (6) implies an ellipsoid and its interior in the m-dimensional space [5]. This ellipsoid is called a force manipulability ellipsoid (FME).

Figure 2 shows a typical 2-link manipulator, where link frames and joint angles θ_1 and θ_2 are defined according to the Denavit-Hartenberg notation. It is assumed that the actuators – motors or brakes - are directly attached to each joint. When the manipulator is driven with active actuators such as electric motors, the endpoint P can generate a

force **F** in any direction in task space (or Cartesian space) and thus a force manipulability ellipsoid (FME) becomes a full ellipsoid. In this case, $\boldsymbol{\tau}$ can be given by

$$\boldsymbol{\tau} = [\cos(\phi) \quad \sin(\phi)]^T \tag{7}$$

where ϕ is an angle between 0 and 2π.

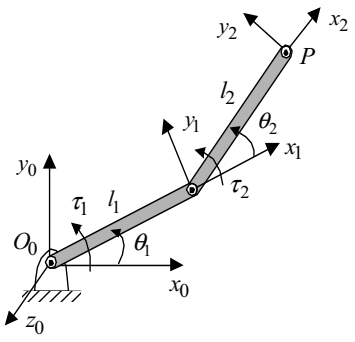

Figure 2. Typical 2-link manipulator

4. Passive FMEs for a 2-link haptic device

The FME (force manipulability ellipsoid) is computed on the assumption that all joints can be fully controllable as in electric motors. How are the FMEs affected for the systems such as tendon-driven mechanisms and passive devices equipped with energy dissipative actuators? Melchiorri investigated the FME for the WireMan, a tendon-driven mechanism [7]. Its FME was obtained using the constrained joint torques and consequently force display was available only in the limited angle range. This means that any desired force placed out of the specified region cannot be appropriately displayed. Some schemes have been developed to increase the region in which force display is available. How will the FME be changed for passive haptic systems? In [7], the FME of a passive system can be drawn using a set of constrained $\boldsymbol{\tau}$ (actually $\boldsymbol{\tau}_C$), which is obtained by applying the passive constraint of Eqs. (3) and (4) to Eq. (7). Investigation of the passive FME can show limitations of passive haptic display at a given configuration and thus lead to good design of a passive haptic device.

Information on $\dot{\mathbf{q}} = [\dot{\theta}_1 \quad \dot{\theta}_2]^T$, $\boldsymbol{\tau}_H$ and $\boldsymbol{\tau}_{Cd}$ is necessary for application of the passive constraint. A desired torque $\boldsymbol{\tau}_{Cd}$ to be displayed can be in any direction because it is determined mainly by a surface normal vector of a virtual wall. An input torque by a human operator $\boldsymbol{\tau}_H$ is determined arbitrarily by a user's will. Thus $\boldsymbol{\tau}_H$ (or $\boldsymbol{\tau}_{Cd}$) can be described by a unit circle (i.e., Eq. (7)). Since each joint velocity can take +, - and zero values, there exist 9 combinations in a 2-link device shown in Fig. 3, which shows combinations of joint velocity in joint and task space. Now consider the case of $\dot{\theta}_1 = 0$ and $\dot{\theta}_2 = 0$, in which $\boldsymbol{\tau}_C$ can be determined only by $\boldsymbol{\tau}_H$ and $\boldsymbol{\tau}_{Cd}$ in Eq. (4). Since $\boldsymbol{\tau}_H$ can have any direction, $\boldsymbol{\tau}_C$ is able to form a unit circle, thus leading to the passive FME with a full ellipsoid as in active actuators.

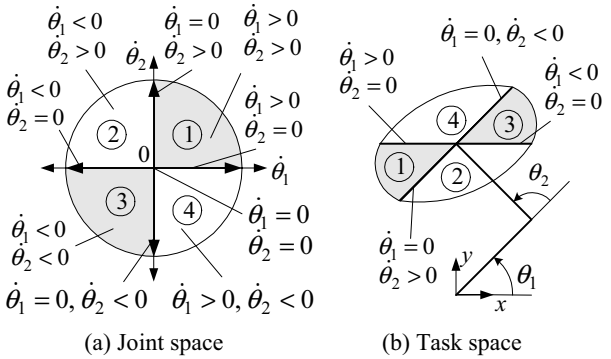

($\theta_1 = 45^o$, $\theta_2 = 90^o$, $l_1 = l_2 = l$)

Figure 3. Combinations of $\dot{\theta}_1$ and $\dot{\theta}_2$

Consider region 1 in Fig. 3 (i.e., $\dot{\theta}_1 > 0$, $\dot{\theta}_2 > 0$). By Eq. (3), $\boldsymbol{\tau}_C$ will be given as $\tau_{C1} \le 0$ and $\tau_{C2} \le 0$. When $\dot{\theta}_1 > 0$ and $\dot{\theta}_2 = 0$, $\tau_{C1} \le 0$ and τ_{C2} is determined only by τ_{H2}, and thus τ_{C2} can have any sign (i.e., +, - or 0). All possible control torques are illustrated for various combinations of joint velocities in Fig. 4 except for the special case of $\dot{\theta}_1 = 0$, $\dot{\theta}_2 = 0$. Region *i* in Fig. 4(a) is computed with region *i* in Fig. 3(a). Note that the shaded sub-regions in Fig. 4(b), (c), (d) and (e) are obtained when one of joint velocities is zero.

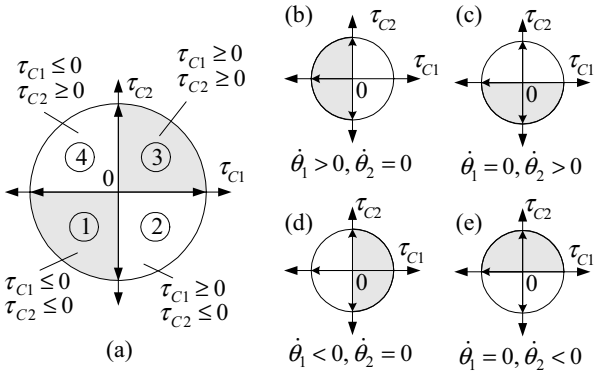

Figure 4. Possible control torques for various combinations of $\dot{\theta}_1$ and $\dot{\theta}_2$

A passive FME can be plotted by transforming $\boldsymbol{\tau}_C$ into the endpoint forces in the task space using the Jacobian relation (i.e., Eq. (5)) as shown in Fig. 5. The boundary of

an FME is drawn from $\| \boldsymbol{\tau}_C \| = 1$. The sub-regions of the passive FME are delimited by four reference forces **A**, **B**, **C**, and **D.** The reference forces are the ones generated when only one brake is applied while another is released. For example, if $\tau_2 < 0$ (or $\tau_2 > 0$) with $\tau_1 = 0$, then force **A** (or **C**) is generated. Likewise, force **B** (or **D**) is generated for $\tau_1 > 0$ (or $\tau_1 < 0$) with $\tau_2 = 0$.

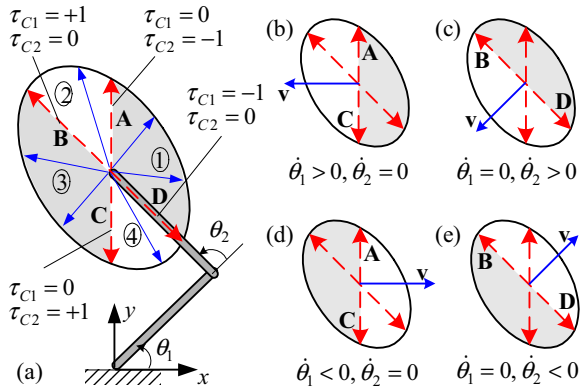

$(\theta_1 = 45^\circ, \theta_2 = 90^\circ, l_1 = l_2 = l)$

Figure 5. Passive FMEs

Note that the inner product of any **v** in region 1 in Fig. 3(b) and **F** in region 1 in Fig. 5(a) is less than zero. This is also obvious from the passive constraint of Eq. (3). Thus a desired force $\mathbf{F}_{Cd}$ for a given end point velocity **v** can be displayed by a passive actuator only when

$$\mathbf{F}_{Cd} \cdot \mathbf{v} \le 0 \qquad (8)$$

Therefore, the constraint of Eq. (8) determines possible regions which can be displayed by passive devices.

In order to examine haptic display capability associated with the passive FME, consider the following situations. Suppose one wants to generate a force in the $+x$ direction (i.e. region 1), while the end point of the manipulator is moving in the $-y$ direction. This motion is possible when $\dot{\theta}_1 < 0$ and $\dot{\theta}_2 > 0$, thus corresponding to region 2 in Fig. 5(a). Therefore, creating a desired force in the $+x$ direction for this motion is not possible since force **A**, the nearest force to the desired force, has 90° with the desired force for a given configuration. Next, suppose the force in the $-x$ direction is needed for the same situation. In this case the angle between force **B** of region 2 and the desired force becomes 45° (< 90°). If force **B** is generated by applying brake 1 alone, the component of this force can be directed in the $-x$ direction and thus the desired force can be roughly displayed, although unnecessary force components are inevitably created in other directions. Thus the desired force can be approximately displayed by force **B**.

Figure 6 illustrates an example of displaying a virtual wall with various configurations. A force $\mathbf{F}_C$ is generated by application of a brake torque $\boldsymbol{\tau}_C$ and $\mathbf{n}_S$ is the surface normal vector of a wall. Suppose that a user wants to move the endpoint along the surface of a virtual wall. The endpoint gets in contact with the wall at position 1 and moves on the surface and then reaches position 2 at the next sample by the action of $\mathbf{F}_C$ and $\mathbf{F}_H$. In this way, displaying a virtual wall is possible by exerting an appropriate force existing in a given passive FME at every sampling instant. But is it always applicable? Even though $\mathbf{F}_C$ (or $\boldsymbol{\tau}_C$) is appropriately generated, one cannot ensure that the endpoint will move along the surface. Action of $\mathbf{F}_H$ is a critical factor to determine motion of the endpoint. This is another type of limitation of the passive device and will be discussed in the next section in detail.

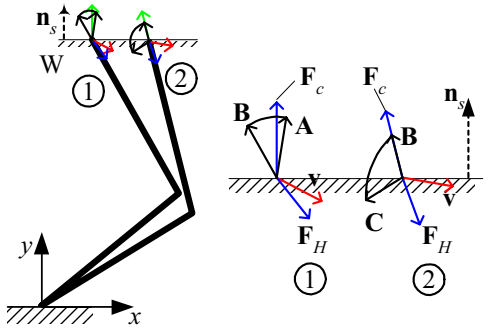

(a) Displaying Virtual (b) Detailed view

Figure 6. Motion on a virtual wall

5. Reference Forces

Haptic display by a passive device was discussed through FME analysis in the previous section. In this analysis a region of possible forces generated by a haptic device was investigated at the particular configuration of the device. In many haptic applications, however, the end point of a device moves along a certain trajectory (i.e., the surface of a virtual wall) and haptic display plays a role of path guide. As mentioned above, one cannot ensure the motion of the endpoint without considering an input force $\mathbf{F}_H$ by a human operator. In this section performance of path guidance of a passive haptic device will be discussed.

Figure 7 illustrates force reflection of the passive device with the identical configuration ($\theta_1 = 45^\circ$, $\theta_2 = 90^\circ$, $l_1 = l_2 = l$) for different virtual walls (i.e., upwards and downwards). $\mathbf{F}_C$ is generated by application of the control torque $\boldsymbol{\tau}_C$, and $\mathbf{v}_r$ is the endpoint velocity created as a result of combined forces $\mathbf{F}_H$ and $\mathbf{F}_C$. $\mathbf{n}_s$ is the surface normal of the virtual wall, which is the direction of a desired force $\mathbf{F}_{Cd}$. In Fig. 7(a) $\boldsymbol{\tau}_{Cd}$ is computed by Eq. (5) using $\mathbf{F}_{Cd}$ whose direction is defined to be the same as $\mathbf{n}_s$ and magnitude is given by the amount of wall deflection. Since $\mathbf{F}_{Cd}$ is in the direction of reference force A that is

part of region 1, so $\boldsymbol{\tau}_{Cd}$ is fully achievable and thus $\boldsymbol{\tau}_C = \boldsymbol{\tau}_{Cd}$ (i.e., $\tau_{C1} = 0$, $\tau_{C2} < 0$ by Fig. 5(a)). Similarly, $\tau_{C1} = 0$, $\tau_{C2} > 0$ in Fig. 7(b). Assume that $\mathbf{F}_H$ is given so that $\tau_{H1} > 0$ and $\tau_{H2} > 0$.

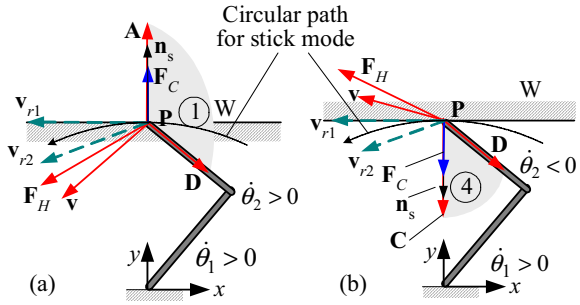

Figure 7. Path guidance on virtual wall

In the actual application of a haptic device in which most operations are performed at low velocities near the wall surface and its inertia is low, its dynamics can be neglected in estimating motion of the device. That is, the endpoint velocity is assumed to change instantly depending on the forces acting on it.

Let us consider the following two cases:

1. $\tau_{H2} = -\tau_{C2}$ in the stick mode

2. $|\tau_{H2}| > |\tau_{C2}|$ in the slip mode

In the stick mode, the endpoint P moves along a circular path (whose origin is joint 1) with joint 2 locked in both cases. The motion direction depends on the sign of $\tau_{H1}+\tau_{C1}$. The resulting velocity of P becomes $\mathbf{v}_{r1}$, and it is tangential to the circular path, so the virtual walls in Fig. 7(a) and (b) can be properly displayed at the given instant. However, we should check where the position of P is placed at the next sampling instant. Since the motion of P is circular, it is expected that the endpoint P will be located inside the wall in Fig. 7(a) and outside the wall in Fig. 7(b) at the next sampling instant.

In the slip mode, the sign of $\tau_{H2}+\tau_{C2}$ should be considered. It is observed that $\tau_{H2} + \tau_{C2} > 0$ (i.e., $\tau_{H2} > 0$, $\tau_{C2} < 0$, $|\tau_{H2}| > |\tau_{C2}|$) in Fig. 7(a) and $\tau_{H2} + \tau_{C2} > 0$ (i.e., $\tau_{H2} > 0$, $\tau_{C2} > 0$, $|\tau_{H2}| > |\tau_{C2}|$) in Fig. 7(b). Since $\tau_{H2} + \tau_{C2} > 0$ in both cases, $\dot{\theta}_2 > 0$. Also $\dot{\theta}_1 > 0$ because $\tau_{C1} = 0$, $\tau_{H1} > 0$ in both cases. Considering the signs of joint velocities, we can expect that the resulting velocity of P becomes $\mathbf{v}_{r2}$.

In Fig. 7(a) the position of P at the next sample will be inside the wall for both stick and slip modes. Therefore, as the path guidance proceeds, the amount of penetration increases, thus leading to increased braking torques. As a consequence, the device will be locked completely, and proper haptic display is impossible. However, in Fig. 7(b) P will be outside the wall for both modes, so such a "locking" problem does not occur.

From the specific example, it is observed that haptic display by a passive device is not always possible, and its performance can be analyzed by observation of reference forces of the FME. Recall that the reference forces are the ones generated when only one brake is in action while another is released in a 2-link manipulator. When one joint is fully locked, the DOF of the corresponding joint is eliminated. A 2-link manipulator would reduce to a single DOF system and thus the locus of its endpoint becomes a circular path. This path was introduced as the Single DOF line in [3] and used for path guidance.

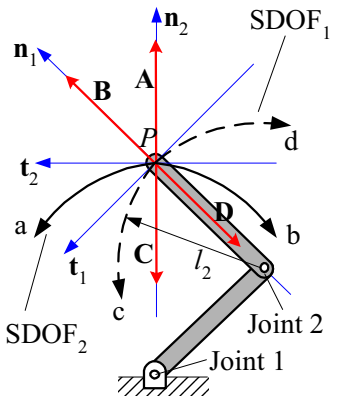

Figure 8. SDOF lines

Consider a guided (or controlled) velocity $\mathbf{v}_r$ of the endpoint P to evaluate performance of path guidance at an arbitrary instant. Two unit vectors $\mathbf{t}_1$ and $\mathbf{t}_2$ along the tangent of the SDOF lines in the case of the 2-link manipulator in Fig. 8 can be defined and $\mathbf{v}_C$ can be expressed as a linear combination of 2 unit vectors

$$\mathbf{v}_r = k_1\mathbf{t}_1(\mathbf{q}) + k_2\mathbf{t}_2(\mathbf{q}) \qquad (9)$$

where k_i is the scalar factor and $\mathbf{v}_r$ is the resulting velocity of the endpoint. $\mathbf{t}_i$ is a unit vector of velocity resulting by $\mathbf{SDOF}_i(\mathbf{q})$, which is the endpoint path at the configuration $\mathbf{q}$ with brake i fully activated (or locked). For instance, $\mathbf{SDOF}_1$ represents a circular path cd at the configuration of $q_1 = 45^o$, $q_2 = 90^o$ in Fig. 8. $\mathbf{t}_1$ and $\mathbf{n}_1$ is the unit vectors along and normal to the tangent of $\mathbf{SDOF}_1$ at the given configuration $\mathbf{q}$, respectively. Eq. (9) is also applicable to active haptic devices. The only difference is that a sign of k_i is determined by the sign of joint velocity or torque in the case of passive devices, while k_i can have any sign for active devices.

An example of path guidance is presented in Fig. 9. W is a virtual wall and $\mathbf{n}_s$ is the surface normal vector of W. When a friction force along the surface is ignored, the desired force to be displayed is in the direction of $\mathbf{n}_s$. When the endpoint velocity $\mathbf{v}$ belongs to region 2 in Fig. 3(b), a force in region 2 of Fig 5(a) is to be displayed. Suppose that a sign of k_i is selected only by τ_{Hi}. From Eq.

(8), $\mathbf{F}_H$ should exist in a region that satisfies $\mathbf{n}_s \cdot \mathbf{F}_H < 0$. In this particular example, the region is divided into three sub-regions which have different k_i. If $\mathbf{F}_H$ is given as $\mathbf{F}_{HA}$, both k_1 and k_2 are positive (i.e., $\tau_{HA1} > 0$, $\tau_{HA2} > 0$). The unit vector $\mathbf{t}_1$ is directed inward while $\mathbf{t}_2$ outward. The guidance is possible due to $\mathbf{t}_2$ in this case. For the case of $\mathbf{F}_{HB}$ ($\tau_{HB1} < 0$, $\tau_{HB2} > 0$), k_1 (or k_2) have the negative (or positive) sign. Both $\mathbf{t}_1$ and $-\mathbf{t}_2$ are directed inward. Thus path guidance cannot be achieved, because motion of the endpoint will be stopped with the maximum action of brakes to account for the increased penetration. Consequently, path guidance is possible unless both $\mathbf{t}_1$ and $\mathbf{t}_2$ are directed toward the inside of a wall.

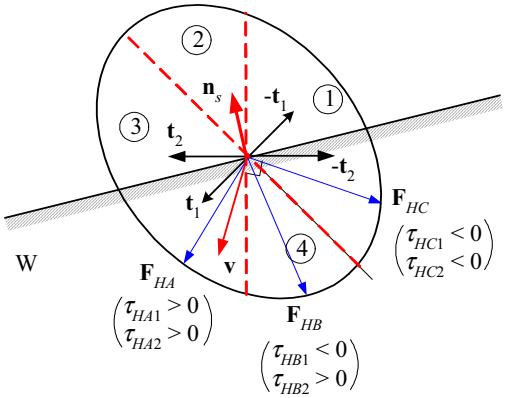

Figure 9. Path guidance for different human inputs

5. Design issues

Limitations on haptic display using electric brakes are discussed in the previous sections. Before dealing with treating design issues in detail, limitations are summarized to evaluate requirements.

1. Limited range of haptic display according to the signs of joint velocities and/or torques given by a user.

2. Conditions for path guidance due to a human input. (i.e., $\mathbf{t}_i$)

As mentioned in Section 4, a desired force is appropriately displayed when $\mathbf{F}_{Cd} \cdot \mathbf{v} \le 0$; otherwise, haptic display is partially achieved or it cannot be conducted at all. It is noted that passive FMEs are delimited by the reference forces. Path guidance performance is affected by $\mathbf{t}_i$ which is generated by the reference forces. Since all limitations mentioned above are related to the reference forces, they are important to performance of a passive haptic device.

The main issue on designing a passive haptic device is how to build reference forces. The more number of reference forces may lead to an increased capability in path guidance, but a haptic device becomes complex accordingly. A kinematically redundant device or a parallel mechanism equipped with redundant actuation can give more reference forces. For example, a 3-link manipulator in [7] had six reference forces in the case of 2 DOF problem in task space and thus could create broader passive FMEs. In the case of a parallel mechanism with redundant actuation, redundant DOFs of actuation will give additional reference forces as the case of a kinematically redundant manipulator. Reference forces have predefined directions by kinematical constraints (i.e., actually **J**) at each instant. How can we control or vary some parameters in kinematic constraints by other inputs? It means that directions of reference forces are adjustable, when parameters in the kinematic constraints are changeable like the scooter in [2].

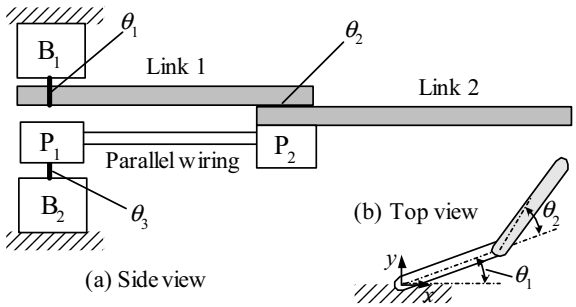

Figure 10. 2DOF coupled wire tendon drive manipulator

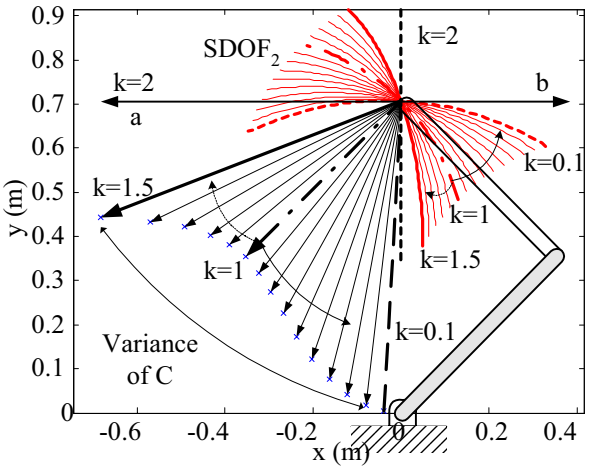

Figure 11. Variations in force direction for change in k

Consider a 2 DOF coupled wire tendon-driven manipulator in Fig. 10. A constraint exists due to the coupled mechanism and can be expressed as

$$\theta_2 = k\theta_3 - k\theta_1 \qquad (10)$$

where k is the reduction ratio between P_1 and P_2. Suppose

k is adjustable with a transmission such as a continuously variable transmission (CVT). Directions of reference forces associated with θ_2 will be changed in order to represent the variance of k as shown in Fig. 11.

6. Conclusions

In this paper a 2-link passive haptic device equipped with electric brakes was discussed. Since passive devices cannot generate forces in all directions, determination of the region available for force reflection was important to their design and operation.

1. A passive force manipulability ellipsoid (FME) can provide a convenient analytical tool for evaluating limitations of a passive haptic display.
2. The limitations revealed that reference forces play an important role in haptic display with energy dissipative actuators and can be used for a design criterion of a passive haptic device.
3. Successful haptic display of a passive haptic device at one instant does not guarantee successful path guidance along the virtual wall.

Currently, development of a 2-link passive haptic device which can overcome limitations mentioned in this paper is under way.

References

[1] B. Hannaford, J.-H. Ryu, "Time Domain Passivity Control of Haptic Interfaces," Proc. of the IEEE Int. Conf. on Robotics and Automation, pp. 1863-1869, 2000.

[2] J. E. Colgate, M. A. Peshkin, W. Wannasuphoprasit, "Nonholonomic Haptic Display," Proc. of the IEEE Int. Conf. on Robotics and Automation, pp. 539-544, 1996.

[3] D. K. Swanson, W. J. Book, "Obstacle Avoidance Methods for a Passive Haptic Display," Proc. of the IEEE Int. Conf. on Advanced Intelligent Mechatronics, pp. 1187-1192, 2001.

[4] C. Cho, M. Kim, J. Song, "2 DOF Passive Haptic Display with Redundant Actuation for Increase in Force Manipulability Ellipsoid," Proc. of the IEEE Int. Symp. on Robotics and Automation, pp. 512 – 518, 2002.

[5] T. Yoshikawa, Foundations of Robotics: Analysis and Control, The MIT Press, 1990.

[6] D. Karnopp, "Computer Similation of Stick-Slip Friction in Mechanical Dynamic System." ASME Journal of Dynamic Systems, Measurement, and Control, Vol. 107, pp. 100-103. 1985

[7] C. Melchiorri, G. Vassura, "A Performance Index for Under-Actuated, Multi-Wire, Haptic Interface," Proc. of the IEEE Int. Conf. on Robotics and Automation, pp. 1026-1031, 1998.

[8] J. Troccaz, S. Lavallee, E. Hellion, "A Passive Arm with Dynamic Constraints: A Solution to Safety Problems in Medical Robots?," Proc. of the Int. Conf. On Systems, Man and Cybernetics, Vol. 3, pp. 166–171, 1993.